Potentiating effects of RAD001 (Everolimus) on vincristine therapy in childhood acute lymphoblastic leukemia

Roman Crazzolara,[1] Adam Cisterne,[1] Marilyn Thien,[1] John Hewson,[1] Rana Baraz,[1] Kenneth F. Bradstock,[2] and Linda J. Bendall[1]

[1]Westmead Institute for Cancer Research, Westmead Millennium, University of Sydney, Westmead; and [2]Department of Haematology, Westmead Hospital, Westmead, Australia

Despite advances in the treatment of acute lymphoblastic leukemia (ALL), the majority of children who relapse still die of ALL. Therefore, the development of more potent but less toxic drugs for the treatment of ALL is imperative. We investigated the effects of the mammalian target of rapamycin inhibitor, RAD001 (Everolimus), in a nonobese diabetic/severe combined immunodeficiency model of human childhood B-cell progenitor ALL. RAD001 treatment of established disease increased the median survival of mice from 21.3 days to 42.3 days ($P < .02$). RAD001 together with vincristine significantly increased survival compared with either treatment alone ($P < .02$). RAD001 induced a cell-cycle arrest in the $G_{0/1}$ phase with associated dephosphorylation of the retinoblastoma protein, and reduced levels of cyclin-dependent kinases 4 and 6. Ultrastructure analysis demonstrated the presence of autophagy and limited apoptosis in cells of RAD001-treated animals. In contrast, cleaved poly(ADP-ribose) polymerase suggested apoptosis in cells from animals treated with vincristine or the combination of RAD001 and vincristine, but not in those receiving RAD001 alone. In conclusion, we have demonstrated activity of RAD001 in an in vivo leukemia model supporting further clinical development of target of rapamycin inhibitors for the treatment of patients with ALL. (Blood. 2009;113:3297-3306)

Introduction

Acute lymphoblastic leukemia (ALL) is the most common malignancy diagnosed in children.[1] Despite intense research, a majority of children who relapse still die of ALL.[2] The development of new treatments for ALL that use more potent but less toxic drugs will therefore be imperative to save more lives.

B-cell progenitor ALL is the most common type of ALL and arises from acquired mutations in early B-cell progenitors.[3] Mutations in ALL result in highly cycling clonogenic cells, which are arrested at the progenitor-cell stage.[3] We and others have demonstrated that the survival and proliferation of ALL cells are dependent on signaling through the p38MAPK, MEK, and PI-3K/AKT pathways.[4-6] Although this represents a simplified chain of events, it points to crucial pathways that could be used as therapeutic targets.

Recently, the mammalian target of rapamycin (mTOR) has received much attention as a potential target in many cancers, including hematologic malignancies.[7-12] mTOR is crucial for the transmission of proliferative and antiapoptotic signals through the PI-3K/AKT transduction pathway.[13] After activation by various growth factors and nutrients, mTOR regulates the G_1 to S phase traverse by phosphorylating 2 proteins important in translational control: the S6 ribosomal protein kinase 1 (p70S6K) and the initiation factor 4E-binding protein 1 (4E-BP1).[14,15] There are increasing clinical data showing promising activity of mTOR inhibitors against solid tumors,[14,15] and RAD001 has been tested in phase 1/2 trials for hematologic malignancies, although ALL was not included in these studies.[11]

In mouse experimental models, mTOR inhibitors acting as single agents have significant antitumor activity.[10,16-18] Furthermore, data are emerging that the combination of mTOR inhibitors and other therapeutic agents is more effective.[8,18] Indeed, synergistic interactions have been demonstrated between mTOR inhibitors and standard chemotherapeutics, such as doxorubicin,[19] as well as with anticancer agents targeting growth factor pathways.[8,20] To date, preclinical studies examining the potential of mTOR inhibitors in combination with standard chemotherapy for the treatment of ALL have not been reported.

In this study, we examined the efficacy of the orally bioavailable mTOR inhibitor, RAD001, on ALL. The effects of RAD001 were analyzed on xenografts established from 5 patients with childhood ALL in a nonobese diabetic/severe combined immunodeficiency (NOD/SCID) mouse model. RAD001 strikingly reduced tumor burden via cell-cycle inhibition and induction of cell death, conferring prolonged survival of engrafted animals. These effects were enhanced by the addition of vincristine, a principal drug incorporated in all current chemotherapy protocols for ALL,[21] thereby proposing RAD001 as an attractive new compound in the treatment of ALL.

Methods

Leukemic cells

Leukemic blasts were obtained from 5 patients (Table 1) with ALL after informed consent was obtained in accordance with the Declaration of Helsinki and institutional ethics committee approval from the Sydney West Area Health Service Human Ethics Committee. Mononuclear cells were

Submitted February 5, 2008; accepted January 8, 2009. Prepublished online as *Blood* First Edition paper, February 4, 2009; DOI 10.1182/blood-2008-02-137752.

The online version of this article contains a data supplement.

The publication costs of this article were defrayed in part by page charge payment. Therefore, and solely to indicate this fact, this article is hereby marked "advertisement" in accordance with 18 USC section 1734.

Table 1. Clinical information

Patient ID	Sex/age, y	Source	Percentage of blasts	Stage	Immunophenotype	Cytogenetics
1345	F/5	BM	95	D	$CD10^+$	45 XX dup(1)(q42 q25), del(3)(q21), −9, del(9)(p22), t(18;20)(q21q13.1)
1999	F/14	BM	94	D	$CD10^+CD34^-$	46 XX
0398	M/15	BM	96	R	$CD10^-CD34^+$	46 XY add(3)(q29) t(14:19)(q32p13)
1196	F/8	BM	NA	D	$CD10^+CD34^-$	46 XX −19,del(19), t(1;19)(q23p13)
2032	M/12	BM	NA	D	$CD10^+CD34^-$	46 XY add (9)(p24), del(9)(p21), del(13)(q11q21), der(19) t(1;19)(q23;p13)

D indicates diagnosis; NA, not available; and R, relapse.

prepared and cryopreserved as described previously.[22] Xenografts were established in NOD/SCID mice as previously described.[23] Cells recovered from the spleens of these animals were used in experiments described here.

Antibodies and reagents

RAD001 was supplied by Novartis Institutes for BioMedical Research, Oncology (Basel, Switzerland). This study used the following antibodies: antihuman CD19-phycoerythrin (4G7), CD19-allophycocyanin (SJ25C1), CD10-fluorescein isothiocyanate (FITC; SS2/36), CD34-peridinin chlorophyll protein (8G12; BD Biosciences, Sydney, Australia); antimurine CD45-FITC (30-F11; Caltag, Mount Waverley, Australia); antiphospho-4E-BP1, anti-4E-BP1, anti-AKT, antiphospho-AKT, anti-poly(ADP-ribose) polymerase (PARP), anti-PTEN, anti-cdk4, anti-cdk6, anti-S6 ribosomal protein (S6RP) antiphospho-S6RP (pS6RP; Cell Signaling Technology, Danvers, MA); antiphospho-retinoblastoma protein (Rb; Abcam, Cambridge, United Kingdom); rabbit antibodies to human LC3, phospho-p38MAPK (T180/Y182), and p38MAPK (Genesearch, Arundel, Australia); horseradish peroxidase (HRP)–conjugated swine anti–rabbit immunoglobulins, FITC-conjugated swine anti–rabbit immunoglobulins (Dako Denmark, Glostrup, Denmark), and mouse anti–β-actin and HRP-conjugated goat anti–mouse immunoglobulins (Sigma-Aldrich, St Louis, MO). Antibodies were used as recommended by the manufacturers.

Mouse models

NOD/SCID mice were housed in sterile micro-isolator cages in ventilated racks. Protocols were approved by the Westmead Animal Ethics Committee. RAD001 was formulated at 2% (wt/vol) in a microemulsion vehicle (Novartis, Basel, Switzerland). RAD001 and vehicle solution were diluted to 1 mg/mL in dH_2O and stored at −20°C; 100 μL of freshly thawed RAD001 (5 mg/kg) or vehicle was given 3 times weekly by gavage. Vincristine (Pharmacia, Sydney, Australia) was diluted to 30 μg/mL in 0.9% saline just before weekly intraperitoneal administration. Mice engrafted with xenografts 1999 and 1345 received 0.15 mg/kg, whereas those receiving remaining xenografts received 0.25 mg/kg. Doses of vincristine were chosen with the intent of obtaining suboptimal responses to the chemotherapy alone and had been previously titrated for xenografts 1999, 1345, and 1196 to obtain a 50% reduction in BM infiltration after 3 weeks of treatment initiated immediately after injection of the cells.

Six- to 8-week-old female NOD/SCID mice received 3 Gy of total body irradiation from an x-ray source delivered by a self-contained cabinet (model X-RAY 320, Precision X-Ray, North Branford, CT; CMS Alphatech, Sydney, Australia), equipped with a Pantak Seifert ISOVOLT 320 HS x-ray tube, 24 hours before administration of 3×10^6 to 5×10^6 human leukemic cells via tail vein injection. Mice were bled weekly, and the percentage of human cells was determined by flow cytometry using antibodies to human CD19 and murine CD45.

In engraftment assays, treatment with RAD001 or vehicle in groups of 5 to 7 mice commenced 24 hours after the injection of ALL cells and continued for 3 weeks before elective death and analysis of tissues. Vincristine was not administered in these experiments.

In survival assays, treatment commenced once more than or equal to 5% leukemic cells were detected in the peripheral blood (PB). Groups of 6 mice received vehicle only, vincristine, RAD001, or both vincristine and RAD001 for 4 weeks. Mouse welfare was assessed daily using standardized score sheets to look for signs of leukemia, including paralysis, loss of weight, ruffled coat, hunched posture, altered respiration, and inactivity. Unless mice unexpectedly died of their disease, a humane endpoint was applied when mice deteriorated in the welfare score. For mice engrafted with xenograft 1999, an elective endpoint was set at 10 weeks after the end of treatment.

In functional assays, treatment was delayed until the mice had an expected survival time of less than 2 weeks. Mice were killed on days 1 and 7 after starting the treatment. PB, bone marrow (BM), and spleens were analyzed for total cell numbers and the presence of leukemic cells by flow cytometry. Spleen cells were collected for flow cytometry and Western blot analysis. Flow cytometry revealed that spleen cells recovered from mice bearing xenografts ALL-1345 and ALL-1999 consisted of 98% (± 0%) and 87% (± 3%) human cells, respectively. Vertebral bodies and sternums were analyzed for ultrastructural changes affecting leukemic cells by light microscopy and transmission electron microscopy (TEM). Livers and femurs were collected for histologic examination.

Pharmacokinetic and pharmacodynamic analyses were performed in mice engrafted with ALL-1345 or ALL-0398 and treatment initiated as described for survival assays. Mice were killed after 0, 2, 4, 7, 24, and 48 hours after a single administration of RAD001 and after 7 and 14 days of 3 times weekly treatments with RAD001. PB was collected by cardiac puncture into ethylenediaminetetraacetic acid for the analysis of RAD001 concentrations or heparin for determination of bilirubin, liver enzymes, and creatinine levels.

Flow cytometry

Flow cytometric analysis of cells labeled with directly conjugated monoclonal antibodies was done as previously described and analyzed on a FACSCanto flow cytometer (BD Biosciences).[23] For cell-cycle analysis, cells were fixed in 80% ethanol after surface labeling for human CD19 and washed with BD Perm/Wash Solution (BD Biosciences PharMingen, San Diego, CA). Fixed cells were resuspended in 100 μL of BD Perm/Wash Solution containing 0.25 μg of 7-amino-actinomycin D and incubated on ice for 60 minutes. The cells were analyzed on a FACSCalibur flow cytometer (BD Biosciences), and data were fitted using ModFit LT cell-cycle analysis software (Verity Software, Topsham, ME).

Immunofluorescence microscopy

Cells were treated as described and labeled with 10 μM Lysosensor Blue DND-167 (Invitrogen, Carlsbad, CA) in RPMI containing 10% fetal calf serum for 30 minutes at 37°C. Cells were resuspended in fresh medium before examination using an Olympus FV1000 confocal laser scanning microscope system, based on an Olympus IX-81 ZDC microscope (Tokyo, Japan), with BP 330- to 385-nm excitation and BA 420-nm emission filters. Images were captured using FV10-ASW 1.7 software (Olympus), and the number of acidic vacuoles in cells were quantitated using ImageJ software (National Institutes of Health [NIH], Bethesda, MD).

Western blotting

A single-cell suspension was obtained from spleens and red cells lysed with 0.155 M NH_4Cl, 10 mM $KHCO_3$, and 0.1 mM ethylenediaminetetraacetic acid (pH 7.5). Cell lysates were prepared, and equal amounts of protein were loaded in each lane of 7.5% or 15% sodium dodecyl sulfate–polyacrylamide gel electrophoresis gels and transferred onto nitrocellulose membranes as previously described.[24] Phosphorylated and total proteins were detected sequentially on the same membrane using specific primary

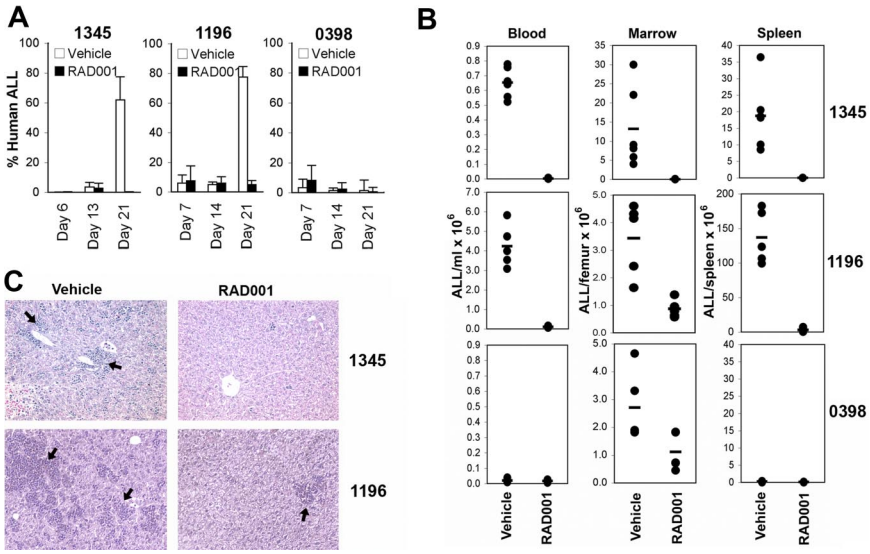

Figure 1. RAD001 inhibits ALL cell engraftment in NOD/SCID mice. NOD/SCID mice, injected with 3 to 5×10^6 cells from indicated xenografts, were treated with RAD001 starting 1 day after the injection of cells. (A) The percentage of human CD19$^+$ cells (mean ± SD) in the PB at weekly bleeds of animals for each group is shown. (B) The total number of human CD19$^+$ cells in the PB, BM, and spleen for each animal at death as determined by flow cytometry. The bar represents the mean of the group. (C) Infiltration of livers with human ALL. Hematoxylin and eosin staining was used. Arrows indicate ALL cells. Original magnification ×200 (details in "Histology"). Larger images are available in Figure S1.

antibodies, appropriate secondary antibodies conjugated to HRP, and enhanced chemiluminescence (PerkinElmer Life and Analytical Sciences, Waltham, MA). Bands were quantitated by densitometry (GE Healthcare, Little Chalfont, United Kingdom) using ImageQuant software.

Electron microscopy

Vertebral bodies and sternums of mice were fixed in modified Karnofsky fixative (2.5% formaldehyde prepared freshly from paraformaldehyde; 2.5% EM grade glutaraldehyde in 0.1 M 3-[N-morpholino]propanesulphonic acid buffer, pH 7.4) and then decalcified in 0.5 M ethylenediaminetetraacetic acid for 14 days. Tissue blocks were trimmed and postfixed in osmium tetroxide, dehydrated in increasing concentrations of ethanol, and embedded in epoxy resin. Semithin (500-nm) sections were cut on a Reichert ultracut microtome and assessed by light microscopy. Ultrathin (80-90 nm) sections were cut and grid stained with 2% ethanolic uranyl acetate and then Reynolds lead citrate. The ultrastructure was examined using a Philips CM-10 transmission electron microscope (FEI, Portland, OR) operated at 80 kV. Images were recorded using Kodak electron microscope film type 4489 (Eastman Kodak, Rochester, NY). Black and white prints were scanned using a Hewlett-Packard scanjet flatbed scanner (Palo Alto, CA), and composite images were compiled using Adobe Photoshop software, version 8 (Adobe Systems, San Jose, CA).

Histology

Femurs and livers were fixed in 10% buffered formalin. Femurs were decalcified for 14 days in 0.5 M ethylenediaminetetraacetic acid (pH 7.4). Decalcified femurs were processed into paraffin; 5-μm sections were cut and stained using hematoxylin and eosin as described previously.[25] Slides were examined by transmission light microscopy using an Olympus BX51 microscope fitted with an UPlanFl 20×/0.5 objective at room temperature. Images were captured using a Spot RT slider camera (Diagnostic Instruments, Sterling Heights, MI) and SPOT Advanced software. Composite figures prepared using Adobe Photoshop software.

Pharmacokinetics and clinical chemistry

RAD001 concentrations were determined in duplicate by high-performance liquid chromatography-electrospray tandem mass spectrometry by SydPath Laboratories (St Vincent's Hospital, Sydney, Australia). Standard noncompartmental pharmacokinetic parameters were derived, including the highest and lowest concentration (C_{max}, C_{min}), and the area under the concentration-time curve (AUC) over the 48-hour dosing interval (calculated by trapezoidal summation; AUC48). Serum aspartate aminotransferase, alanine aminotransferase, bilirubin, and creatinine were determined by routine laboratory testing at Institute for Clinical Pathology and Medical Research, Westmead Hospital (Westmead, Australia).

Statistics

Comparisons between 2 groups were performed using Student *t* tests and between multiple groups using analysis of variance. Log transformation was made before analysis to stabilize for variance. Pairwise comparisons between groups were adjusted for multiple comparisons using the Bonferroni method. Linear regression was used to determine correlations between variables. Survival was measured from the onset of disease until death and analyzed using SPSS, version 15.0 (SPSS, Chicago, IL). The Kaplan-Meier method was used to construct survival curves, and results were compared using the log-rank test of survival distribution by treatment stratified by cell line. The number of cells containing acidic vacuoles was compared between groups using Student *t* tests and comparison of the number of acidic vacuoles/cell analyzed using the Kruskal-Wallis test, to determine differences between treatments, and the Jonckheere-Terpstra test to demonstrate association between increasing numbers of AV/cell with increasing concentrations of RAD001.

Results

RAD001 improves survival of NOD/SCID mice engrafted with ALL

We have previously demonstrated the inhibition of ALL engraftment in NOD/SCID mice after blockade of CXCR4/CXCL12[23] and shown that PI-3K/AKT signaling is important for spontaneous and CXCL12-induced ALL cell proliferation in vitro.[6] Therefore, we investigated the effect of inhibition of mTOR, which is downstream of AKT, on ALL engraftment using our established NOD/SCID xenograft model. NOD/SCID mice were treated with the mTOR inhibitor, RAD001, starting the day after the injection of ALL-1345, -1196, or -0398 cells. RAD001 treatment prevented disease progression as determined by weekly assessment of the percentage of leukemic cells in the PB of the 2 xenografts (1345 and 1196) where significant numbers of human cells were detected within the 3-week period (Figure 1A). At death on day 21, significantly fewer ALL cells were present in the BM of RAD001-treated mice for all 3 xenografts and in the spleens and blood of xenografts 1345 and 1196 (Figure 1B). For xenograft ALL-1345, leukemic cells were below the limit of detection (< 0.01%) in the spleens of 5 and the blood of 4 of the 7 treated mice. Similarly, there was

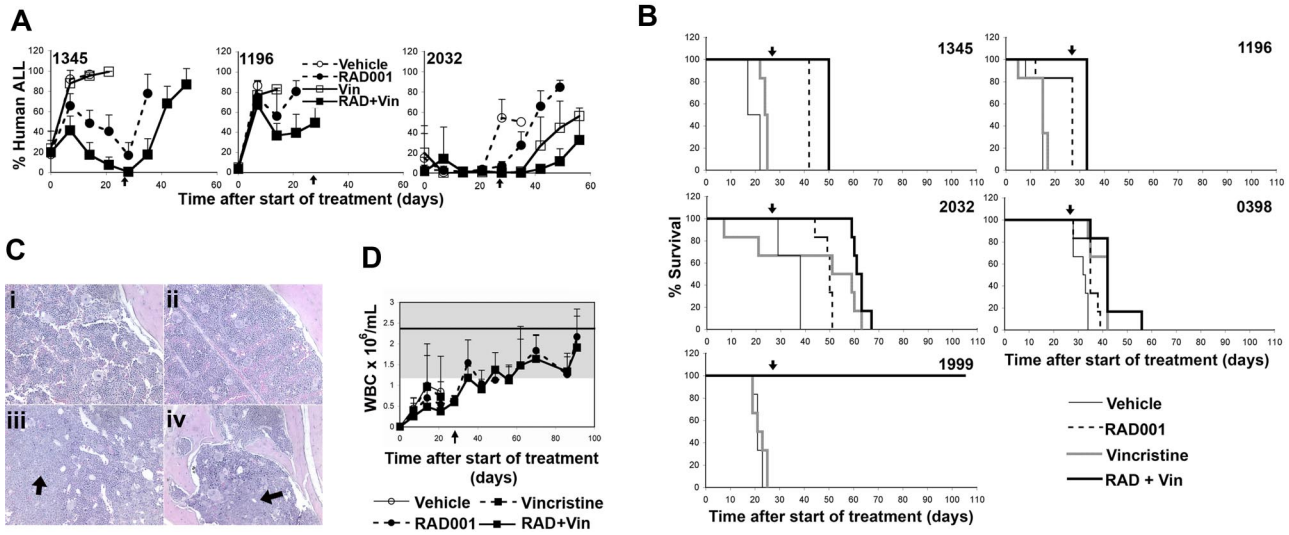

Figure 2. RAD001 improves survival of NOD/SCID mice engrafted with ALL. (A) Percentage of human ALL cells in the blood of mice engrafted with the indicated samples over time. Mice were treated with vehicle, vincristine (Vin), RAD001, or RAD001 and vincristine (RAD + Vin). The time indicated is from the commencement of treatment, and the arrow indicates the completion of treatment. Mean plus or minus SD of surviving animals is shown. (B) Kaplan-Meier plots of the survival of mice engrafted with xenografts from 5 patients with childhood ALL. The time indicated is from the commencement of treatment, and the arrow represents the completion of treatment. (C) Femur (i-iii) or vertebral body hematoxylin and eosin–stained sections (iv) from mice engrafted with ALL-1999 10 weeks after the completion of treatment with RAD001 (i,iii,iv) or RAD001 + vincristine (ii). Subpanels i and ii show normal hematopoiesis, whereas subpanels iii and iv are from the single animal showing disease relapse at the time of death. Regions of leukemic infiltration are indicated by arrows. Original magnification ×200 (details in "Histology"). Larger images available in Figure S2. (D) Murine white blood cell counts (mean ± SD) of surviving NOD/SCID mice engrafted with ALL-1999 during and after the completion of treatment. Time is from the initiation of treatment and the end of treatment indicated by the arrow. The white cell counts were very low at the start of treatment because the mice were still recovering from the sublethal radiation administered to facilitate ALL engraftment. The shaded area represents the normal range; line, mean value for white blood cell counts observed in our NOD/SCID mouse colony. Note that the vehicle- and vincristine-treated mice had all died of disease by day 20.

a dramatic reduction in the degree of ALL infiltration in the livers of RAD001-treated mice bearing xenografts ALL-1345 and -1196 compared with control-treated animals (Figure 1C). Xenograft ALL-0398 did not significantly infiltrate the liver at the time point examined (data not shown). These data demonstrate that RAD001 dramatically inhibits ALL cell engraftment in vivo.

Because of the potent effects of RAD001 in an engraftment setting, we investigated the efficacy of RAD001, alone and in combination with vincristine in established ALL. Five established xenografts were studied. Treatment with RAD001 and/or vincristine began after leukemia was engrafted and disseminated in the PB (> 5% human ALL cells) and continued for 4 weeks, a time consistent with induction protocols. The percentage of leukemic cells in the PB of vehicle-treated animals continued to rise throughout the treatment period until death resulting from disease progression (Figure 2A and data not shown). RAD001 decreased leukemic burden in ALL-1999, -1345, and -2032, stabilized disease in ALL-1196, and had no effect in ALL-0398. Despite low cytotoxicity of vincristine alone, the combination with RAD001 further improved the rate of regression over those observed with RAD001 alone in all samples examined, suggesting interplay between the 2 compounds (Figure 2A and data not shown). Surprisingly long-term complete remission was persistent in ALL-1999 with a rate of 83% and 100%, for single and combined treatments, respectively, 10 weeks after the end of treatment.

The impact of treatment on ALL expansion and dissemination was reflected in the improved overall survival of animals. The median survival of vehicle-treated mice was 21.3 days (range, 13.8-35.0 days) after leukemia was detected in the PB for all 5 ALL xenografts (Figure 2B). RAD001 significantly increased survival for each xenograft with a median survival of 42.0 days (range, 24.5- > 104 days, $P < .02$ using a log-rank test of survival distribution by treatment). As anticipated from the doses selected, vincristine as a single agent enhanced survival in only 2 xenografts (ALL-1345 and -0398) with no overall increase in survival (median survival, 24.1 days; range, 14.0-39.5 days, $P =$ not significant). Despite this, the combination of RAD001 and vincristine enhanced overall survival to a greater extent than treatment with RAD001 (4 of 5) or vincristine alone (3 of 5) with a median survival of 50.0 days (range, 33.0- > 105 days), which was 8 days greater than the survival induced by RAD001 alone and 25.9 days longer than mice receiving vincristine alone ($P < .02$). Detailed statistical analysis of survival data for each xenograft is given in Table 2. In one xenograft (ALL-1999), all RAD001 and RAD001 and vincristine-treated animals survived for 10 weeks after the completion of treatment. Mice were electively culled at this time. Leukemia was detected in only one mouse receiving RAD001 as a single agent. However, the disease was below the limit of detection in all

Table 2. Statistical analysis of survival in response to individual treatments and treatment combinations

Xenograft	RAD001 vs placebo	Vincristine vs placebo	RAD001 + vincristine vs RAD001 alone	RAD001 + vincristine vs vincristine alone
1345	.001	.003	.001	.001
1196	.020	.325	.001	.001
2032	.001	.151	.001	.068
0398	.009	.002	.004	.286
1999	.001	.393	.317	.001

The significance values shown were determined using a Mantel-Cox log rank test.

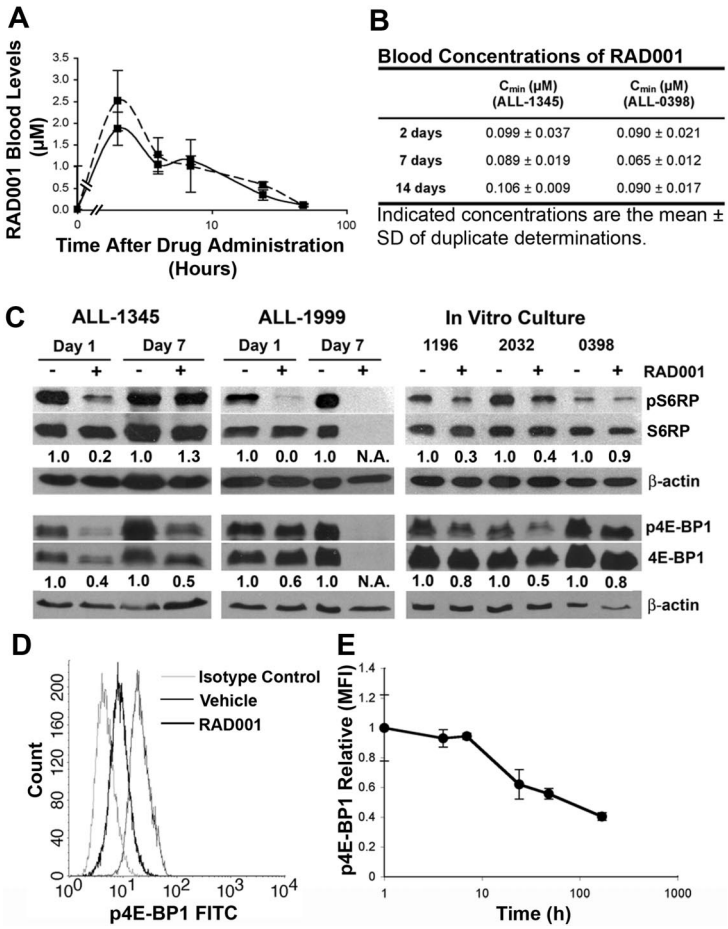

Figure 3. RAD001 concentrations and inhibition of phosphorylation of S6RP and 4E-BP1 after drug administration. Mice engrafted with ALL-1345 or ALL-0398 cells were treated with RAD001 or vehicle and blood harvested after the indicated time points of continuing treatment and evaluated for RAD001 concentrations. (A) RAD001 (mean ± SD, n = 3) concentration-time profiles in mice engrafted with ALL-1345 (—) and ALL-0398 (····) up to 48 hours after administration of a single dose of RAD001. (B) RAD001 (mean ± SD, of duplicate determinations from 3 experiments) trough concentrations in mice treated for up to 14 days with RAD001. (C) Ex vivo analysis of the phosphorylation of S6RP and 4E-BP1 in ALL cells from spleens recovered from mice engrafted with ALL-1345 or ALL-1999, 1 or 7 days into the treatment protocol (left and center panels). Cells from xenografts ALL-1196, -2032, and -0398 recovered from untreated mice were treated in vitro for 24 hours with or without 2 μM RAD001 (right panel). The numbers below the blots indicate the intensity of phosphorylation-specific bands for 4E-BP1 and S6RP relative to total 4E-BP1 and S6RP. (D) Representative plots showing the levels of phosphorylated 4E-BP1 assessed by flow cytometry in ALL cells recovered from spleens of mice engrafted with ALL-1345. (E) Time course of the reduction of phosphorylated 4E-BP1 after administration of RAD001 measured by flow cytometry in ALL cells recovered from mice engrafted with ALL-1345.

hematopoietic compartments in all mice receiving vincristine and RAD001 (Figure 2C and data not shown). Femur sections revealed the return of normal hematopoiesis, and murine blood counts showed white cell counts, hemoglobin concentration, and platelet counts returning to within the normal range in animals receiving RAD001 or RAD001 and vincristine (Figure 2D and data not shown). This suggests that mice recovered well from both their disease and the treatments received. Overall, these data confirm the potent inhibitory effect of RAD001 on the expansion of ALL in vivo and show an interactive effect when combined with the chemotherapeutic agent vincristine.

Tolerance of RAD001 in mice engrafted with ALL

To determine whether the therapeutic effect of RAD001 was dependent on mTOR inhibition in our NOD/SCID model of childhood ALL, systemic exposure to RAD001 was quantified. Peak plasma concentrations of 1.86 plus or minus 0.38 μM (mean ± SD; n = 3) and 2.51 plus or minus 0.69 μM (mean ± SD; n = 3) were achieved 2 hours after a single orally administered dose in NOD/SCID mice engrafted with ALL-1345 and -0398, respectively (Figure 3A). The $t_{1/2}$ was approximately 10 hours. Repetitive administration (3 times weekly) of RAD001 maintained similar trough blood concentrations at days 2, 7, and 14 (Figure 3B). Despite the higher than anticipated blood concentrations, RAD001 was well tolerated in animals engrafted with ALL. There was no consistent trend or finding with respect to several biochemical assessments during the course of the study, in particular serum renal or liver function tests (Table S1, available on the *Blood* website; see the Supplemental Materials link at the top of the online article). Indeed, mice engrafted with ALL-1345 showed elevated alanine aminotransferase levels that were significantly attenuated by RAD001 treatment, reflecting reduced ALL cell infiltration of the liver. In addition, nonengrafted mice treated with RAD001 showed no signs of cytotoxicity or cell degeneration in the hematopoietic cell compartment, with normal reconstitution of the white blood cell counts after sublethal irradiation (data not shown).

RAD001 attenuates phosphorylation of 4E-BP1 and S6RP in ALL cells

To confirm that RAD001 is acting on target, we examined the phosphorylation status of the mTOR target proteins 4E-BP1 and S6RP as well as the nontarget proteins AKT and p38MAPK. For xenografts ALL-1999 and -1345, this was performed on human ALL cells recovered from the spleens of mice after 24 hours of treatment. In xenograft ALL-0398, the purity and quantity of the human cells recovered from the spleens were insufficient for analysis. The remaining xenografts (ALL-1196, -2032, and -0398) were analyzed after a 24-hour in vitro culture in the presence or absence of 2 μM RAD001 based on the peak plasma levels obtained in the mice after oral administration. In the 2 in vivo cases, phosphorylated 4E-BP1 and S6RP were significantly reduced after 24 hours of RAD001 treatment. Samples analyzed after in vitro culture revealed a similar reduction in phosphorylated 4E-BP1 and S6RP after incubation with 2 μM RAD001 (Figure 3C). In ALL-0398, the reduction in phosphorylation was less than that observed in the other samples, a finding consistent with the reduced efficacy of RAD001 in this xenograft. Consistent with the data

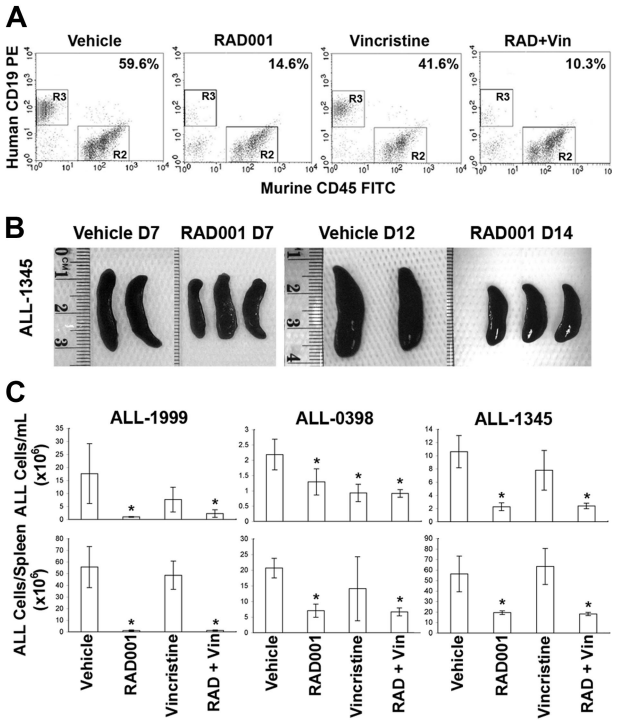

Figure 4. Reduction of ALL cells in the blood and spleens of mice engrafted with human ALL and treated with RAD001, vincristine, or the combination of both for 7 days. Mice engrafted with ALL-1999, -1345, or -0398 were treated with vehicle, RAD001, vincristine, or RAD001 plus vincristine for 7 days. (A) Representative flow cytometric analysis showing the percentage of human ALL cells in the PB of mice engrafted with ALL-1345. The percentage human ALL cells is shown. (B) Photographs of spleens recovered from mice engrafted with ALL-1345 after the indicated days of treatment with RAD001 or vehicle. (C) The absolute number of human ALL cells in the PB and spleens of mice treated as indicated are shown. Bars represent the mean plus or minus SD of groups of between 2 and 4 mice. $^*P < .05$ compared with vehicle-treated animals.

observed by Western blotting, flow cytometric assessment of the phosphorylation of 4E-BP1 on ALL-1345 cells obtained from spleens confirmed similar reductions (Figure 3D,E). On day 7, ALL-1345 no longer demonstrated reduced phosphorylation of S6RP, although phosphorylation of 4E-BP1 was still suppressed. Analysis of total proteins revealed that total 4E-BP1, and in ALL-1999, S6RP protein was also reduced in response to RAD001 in the xenografts on day 7, a finding consistent with the mTOR inhibitor CCI-779.[10] In contrast, no consistent effects on the phosphorylation of AKT or p38MAPK were observed (Figure S3).

Mechanisms underlying improved survival of mice engrafted with ALL receiving RAD001

To determine the mechanisms underlying the reduction of leukemia in vivo, we examined cells recovered from animals engrafted with ALL-1345, -1999, and -0398, which had high tumor burden and had been treated as described in "Methods" for survival experiments for 24 hours or 7 days. One-way analysis of variance was used to analyze the effect of treatment separately in each ALL xenograft because analysis of variance identified a significance of treatment by cell line interaction ($P = .009$). Treatment with RAD001 and/or vincristine did not significantly reduce ALL cell number after 24 hours. However, after 7 days of treatment, RAD001 and the RAD001/vincristine combination reduced the extent of the disease in the PB and spleens of all 3 xenografts compared with placebo-treated animals (Figure 4). No significant effect on the number of ALL cells was observed in the BM at any time point. As observed in childhood ALL patients with high initial leukemic burden, day 7 might be too early to detect a reduction of ALL infiltration in the BM.[26] These data demonstrate that, in the 3 xenografts studied, 7 days of treatment with RAD001 alone or in combination with vincristine, resulted in a reduction in the level of ALL in the animals.

Inhibition of mTOR is known to induce cell cycle arrest in tumor cells, making it possible that RAD001 could be inhibiting ALL expansion in the mice by inhibiting proliferation.[27] Cell cycle analysis performed on cells recovered from the spleens of engrafted mice 24 hours after drug administration revealed that RAD001 induced a $G_{0/1}$ arrest in all 3 xenografts examined (Figure 5A,B). The increase of cells in $G_{0/1}$ was accompanied by a loss of cells in S phase. Vincristine induced a significant G_2/M arrest in ALL-0398 only. The changes in quantitative DNA staining by flow cytometry could be confirmed in the loss of mitotic figures in femoral sections of RAD001-treated animals (Figure 5C). Similar effects on cell cycle status were apparent in cells recovered after 7 days of treatment with complete loss of the G_2/M population in ALL-1345 (data not shown). Western blotting revealed that RAD001, or RAD001 and vincristine, treatment for 24 hours reduced the level of phosphorylated Rb and the level of cyclin-dependent kinase (cdk) 4 and cdk6 in ALL cells isolated from spleens of mice engrafted with ALL-1345 and -1999 (Figure 5D). This effect was consistent with the arrest of ALL cells in $G_{0/1}$ and the reduction of ALL cells observed in PB and spleens after 7 days of treatment with RAD001 (Figure 4).

Mechanisms of RAD001-induced cell death

To determine the mechanisms involved in RAD001-mediated cytoreduction of ALL xenografts, histologic analysis of microenvironmental niches at the endosteum of vertebral bodies of the lower spine was performed. TEM revealed that, consistent with the light microscopy, vincristine treatment resulted in patchy cellular apoptosis, the ultrastructure of which was characterized by uniformly electron dense round nuclear chromatin bodies associated with early preservation of the cytoplasmic membrane and organelles (Figure 6B). In contrast, RAD001 treatment showed only occasional apoptotic cells (Figure 6C). However, a small but significant number of leukemic cells showed double-walled peripheral cytoplasmic polyphagic vacuoles (Figure 6E-G, Figure S5). These vacuoles contained a mixture of complex structures consistent with mitochondria, rough endoplasmic reticulum, polyribosomes, lysosomes among other organelles in various stages of breakdown. The combination of RAD001 and vincristine (Figure 6D) produced both sets of features (ie, the presence of both apoptotic cells and cells containing autophagic vacuoles). This ultrastructure data suggest the induction of autophagy, but not apoptosis, by RAD001.

Induction of apoptosis by vincristine was confirmed by the detection of increased PARP cleavage in lysates of spleen cells recovered from mice receiving vincristine or RAD001 plus vincristine, but this was not observed in those receiving RAD001 (Figure 7A). Cleavage of caspases could not be detected in cells recovered from mice. However, cleaved caspase 3 was detected in the ALL cell line NALM6 after in vitro exposure to vincristine, but not in cells incubated with RAD001. These cells also demonstrated the same pattern of PARP cleavage (ie, only increased in response to vincristine) as had been observed in cells recovered from the mice, although PARP cleavage was more pronounced after in vitro culture (Figure 7B).

The induction of autophagy by RAD001 was further supported by the detection of increased proportion of cells containing acidic

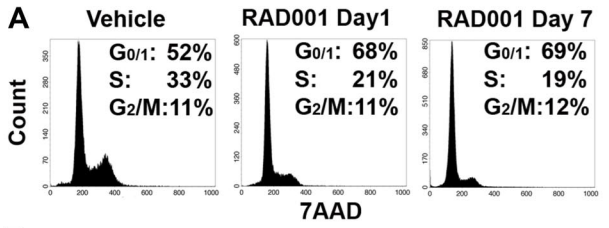

B

Patient No.	$G_{0/1}$ (%)				S (%)				G_2/M (%)			
	Vehicle	RAD001	Vin	RAD+ Vin	Vehicle	RAD001	Vin	RAD+ Vin	Vehicle	RAD001	Vin	RAD+ Vin
1345	53±4	68±5*	56±12	70±8*	33±2	21±12	29±5	15±7*	14±3	11±9	16±7	15±6
1999	53±3	64±5*	56±5	70±5*	41±4	22±2*	36±6	15±4*	7±4	14±3*	7±3	15±3*
0398	68±2	74±1*	68±7	69±3	27±2	19±2*	12±6*	19±3*	5±2	7±1	20±2*	12±5*

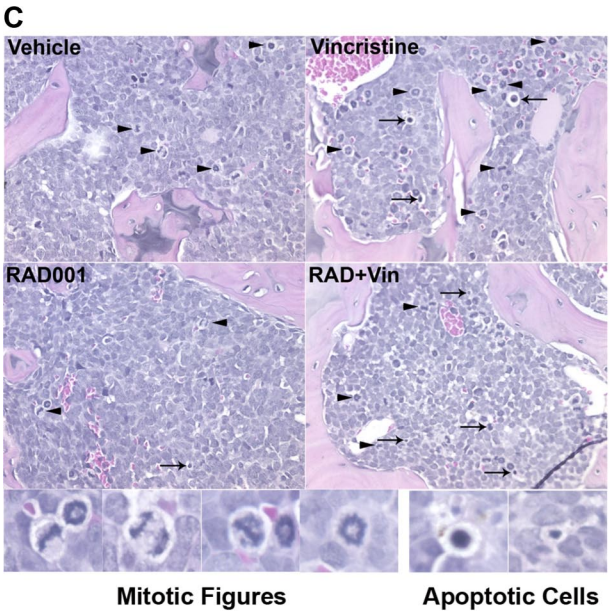

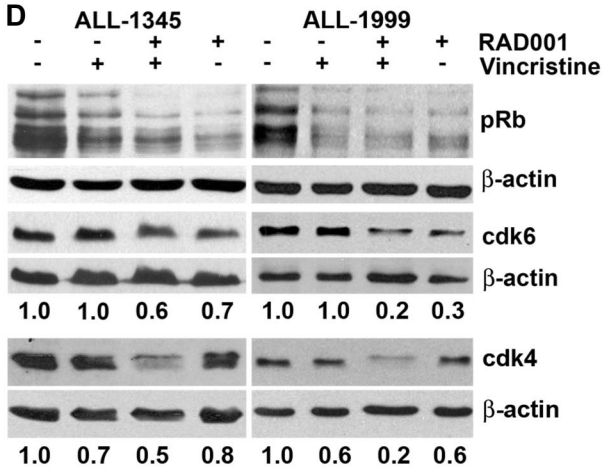

Figure 5. RAD001 arrests ALL cells in G_0/G_1 phase of the cell cycle. Mice were treated with vehicle, RAD001, vincristine, or RAD001 plus vincristine for 1 or 7 days. (A) ALL cells isolated from spleens were labeled with 7-amino-actinomycin D and analyzed by flow cytometry. Cell-cycle profiles of ALL-1345 are shown as representative examples. (B) The percentage of cells in each stage of the cell cycle after 1 day of treatment as indicated is shown. The mean plus or minus SD of the percentage of cells in each cell phase from replicate mice is shown ($n \geq 4$). (C) Hematoxylin and eosin–stained sections from femurs of mice engrafted with ALL-0398 are shown with examples of mitotic (➤) and apoptotic (➵) figures. Original magnification ×200 (details in "Histology"). Higher-power examples of mitotic and apoptotic figures produced by a further 20× digital enlargement are shown below. Larger images available in Figure S3. (D) Effect of RAD001 and/or vincristine treatment on the phosphorylation status of Rb and the levels of cdks 4 and 6 after 1 day of treatment of NOD/SCID mice engrafted with ALL-1345 or ALL-1999. The numbers below the plots indicate the ratio of cdk4 and 6 to β-actin.

vacuoles, and an increase in the number of acid vacuoles detected in each cell ($P < .001$ in all 3 experiments), in response to RAD001 treatment in the ALL cell lines NALM6 and REH (Figure 7D-F). A positive association between the number of acidic vacuoles and the dose of RAD001 applied to the cells was apparent ($P < .001$). Western blotting also revealed an increase in the autophagy-associated protein Beclin-1 and the processing of LC3 to the lipidated form (LC3-II), which associates with autophagosomes (Figure 7C).[28] Overall, the data demonstrate that apoptosis is not the major mechanism of cell death induced by RAD001 alone and is consistent with the picture observed by electron microscopy implicating autophagy as the predominant form of RAD001-induced cell death.

Discussion

Despite significant improvements in primary therapy, long-term outcomes after relapse remain poor, with a 15-year overall survival of only 37% among patients enrolled in the ALL-BFM-87 series of studies.[2] Patients who have a second BM relapse have a 5-year survival of only 8%.[29] Considering the poor outcome, there is a critical need for new drugs with novel mechanisms of action to improve or even prevent relapse of ALL. Complete response rates using familiar reinduction protocols can be as high as 40%, making recruitment into trials of new agents, which often have similar predicted outcomes and increased potential toxicities, difficult.[2] One strategy to improve access onto phase 1 trials in pediatric ALL is to identify new drugs that probably enhance leukemia killing by standard multidrug reinduction regimens, but with minimal added systemic toxicity. With the latter philosophy in mind, we have examined the potential of RAD001, a small orally bioavailable mTOR inhibitor, to treat leukemia as a single agent and as a combinational agent with vincristine, a widely used agent of multimodal chemotherapy in several study groups.

The primary goal of this study was to provide preclinical data to form a rational basis for combining mTOR inhibitor therapy with conventional cytotoxic agents. Thus, we adapted RAD001 treatment regimens of animal experiments in other tumor types[20,30] to our model of ALL. RAD001 was rapidly absorbed, and consistent

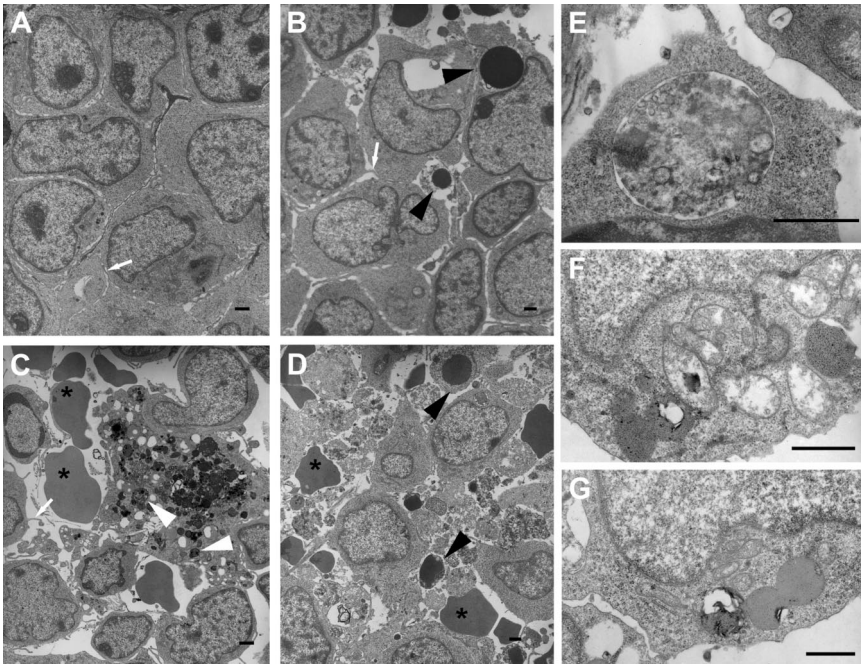

Figure 6. RAD001 promotes autophagy and induces apoptosis. Ultrastructural analysis by TEM of ultrathin BM sections in mice treated with vehicle (A), vincristine (B), RAD001 (C), and vincristine plus RAD001 (D). Apoptotic cells (➤), extravasated erythrocytes (*), filipodia (white arrows), and phagolysosomes (white arrowheads) are indicated. Double-walled polyphagic vacuoles in the cytoplasm of ALL cells from ALL-1345 (E) and ALL-1999 (F,G) recovered from mice treated with RAD001. Bars represent 1 μm. See "Electron microscopy" for details. Larger images are available in Figure S4.

steady-state concentrations in the low to mid nanomolar range were achieved. This is consistent with animal data but contrasts with human studies where increasing blood concentrations are observed over the first days of treatment.[31] The clearance of RAD001 was approximately 4 times faster in ALL-engrafted mice compared with healthy human volunteers,[32] but the overall bioavailability was comparable based on dose-adjusted AUC after a single dose.[32] This was surprising because a considerably lower bioavailability of RAD001 has been previously reported in rats.[33] The high blood trough concentration achieved may be explained by the very high binding (> 99%, Novartis) of RAD001 to plasma proteins in mice, limiting the amount of drug available to enter cells. As a result, mice in this study had a higher RAD001 exposure than pediatric patients in transplantation trials, but the drug concentrations were well tolerated, with no toxicity observed with respect to several biochemical and hematologic assessments, and were comparable with previous in vitro IC_{50} values of survival inhibition and cell death induction of different tumor types to RAD001.[27,34]

Applying our treatment regimen of 3 times weekly administration of RAD001 in 5 ALL xenograft cases, we present convincing evidence of significant inhibition of leukemic growth. The NOD/SCID mouse model more closely reflects disease progression in pediatric patients because leukemic cells disseminate in extramedullary organs, such as spleen and liver, once the BM is engrafted.[35] Treatment with RAD001 inhibited engraftment of ALL in BM and extramedullary organs. RAD001 produced significant reductions in ALL once leukemia was established, resulting in prolonged survival. Notably, in xenografts of ALL-1999, sustained remission with recovery of normal hematopoiesis was demonstrated in 5 of 6 mice up to 10 weeks after finishing RAD001 treatment. Strikingly, we observed a positive interaction between RAD001 and vincristine in the majority of xenografts tested. Because responses of human ALL xenografts to chemotherapeutic agents, such as vincristine, correlate significantly with patient outcome,[36] the enhanced antileukemic activity of RAD001 in a multiagent combination regimen observed in xenografts may predict similar activity in patients. Indeed, another mTOR inhibitor, CCI-779, was similarly shown to enhance the efficacy of methotrexate using a similar model system.[37]

Despite clear and potent effects of RAD001, considerable variation was observed between the responses of the 5 xenografts studied. Loss of PTEN and subsequent constitutive phosphorylation of AKT results in resistance to chemotherapy in ALL, which can be overcome by inhibition of mTOR.[38-40] In addition, RAD001 can paradoxically increase AKT phosphorylation in some malignant cells resulting in resistance to mTOR inhibitors.[41] However, the PTEN protein was present at similar levels in all 5 xenografts (data not shown), and there was no evidence of increased AKT phosphorylation in the ALL cells recovered from either RAD001-treated mice or after 24 hours of in vitro culture with 2 μM RAD001 (Figure S3). Therefore, the variation in responses cannot be explained by alterations in PTEN expression or AKT phosphorylation.

We report here that levels of phosphorylated 4E-BP1 and S6RP were decreased after RAD001 treatment, consistent with current studies on mTOR signaling.[8] RAD001-induced inhibition of cell cycle progression in vivo was associated with reduced levels of phosphorylated Rb, and cdk4 and 6 levels, consistent with previous reports of mTOR inhibition in other cell types.[42-44] Surprisingly, we did not detect increased levels of apoptosis in response to RAD001 treatment, although this was evident after exposure to vincristine. This contrasts with previous reports that mTOR inhibition with rapamycin induces apoptosis in ALL cells.[7,45] The most probable explanation for this discrepancy is the examination of patient ALL cells cultured in vitro in these studies. Under these conditions, ALL cells undergo significant spontaneous apoptosis, which mTOR inhibition may have enhanced, whereas in our study, cells were either recovered ex vivo or were continuous cell lines where spontaneous apoptosis is minimal. However, ultrastructural analysis demonstrated the presence of autophagic vacuoles as well as limited apoptosis in vertebral bodies infiltrated with ALL cells after RAD001 treatment. The clear specific induction of autophagic vacuoles, the induction of Beclin-1, and lipidation of LC3 after RAD001 exposure raise the possibility that ALL cells are dying as a result of excessive autophagy. Although mTOR inhibition is well known to induce autophagic cell death in other cell types,[46] our current data fall short of providing a causal link between the increased autophagy and reduced viability in our model of ALL. However, the successful induction of prolonged

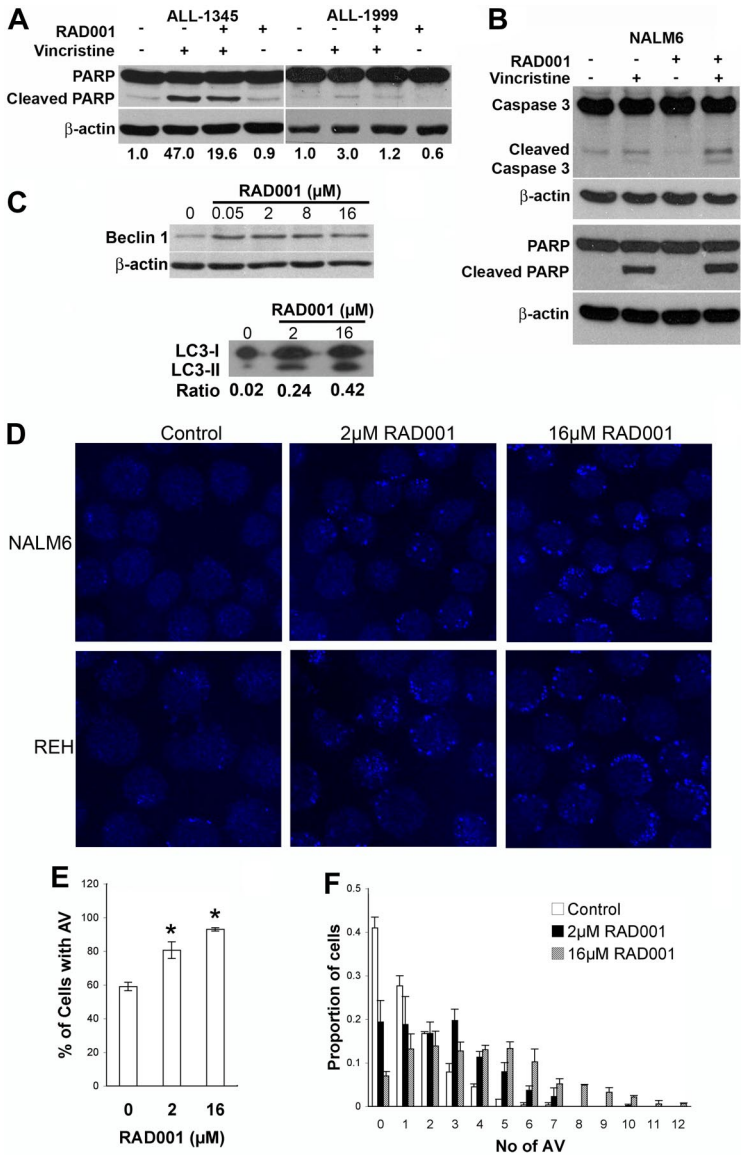

Figure 7. Mechanisms of cell death induced by RAD001 and vincristine alone and in combination. (A) Mice engrafted with ALL-1345 or ALL-1999 cells were treated with vehicle, vincristine, RAD001, or RAD001 plus vincristine for 24 hours and lysates prepared from recovered spleen cells. Lysates were subjected to Western blotting with anti-PARP, or anti–β-actin antibodies. (B) NALM6 cells were cultured with 2 μM RAD001, 1 nM vincristine, or the combination of both for 24 hours and cell lysates prepared. Lysates were subjected to Western blotting with anti-PARP, anticaspase 3, or anti-β-actin antibodies. (C) NALM6 cells were treated with the indicated doses of RAD001 for 24 hours, and cell lysates were analyzed for Beclin-1 and LC3 expression by Western blotting. β-actin is shown as a loading control for Beclin-1, and the ratio of LC3-II/LC3-I is indicated below the blots for LC-3. NALM6 or REH cells were treated with vehicle alone (Control), or 2 or 16 μM RAD001 for 24 hours. Cells were stained for acidic vacuoles using Lysosensor Blue. Representative fields of view are shown in panel D. Original magnification ×600. See "Immunofluorescence microscopy" for details. The proportion of cells containing acidic vacuoles (AV) (E) and the number of AV in each cell (F) are shown. Quantitation was obtained from the analysis of more than 120 cells for each condition in each of 2 separate experiments. The mean plus or minus SD of the independent experiments is shown for NALM6 cells.

remissions in animals with extensive disease suggests that, in the absence of apoptosis, autophagy is a plausible alternative death mechanism. Enhancement of autophagy through mTOR inhibition might be of particular interest for the treatment of ALL because resistance to current chemotherapies has been linked to defects in their apoptotic machinery.[47] Therefore, targeting the nonapoptotic pathway may yield better clinical outcomes for patients undergoing cytotoxic cancer therapies.[48,49]

In conclusion, we have shown that RAD001 can effectively inhibit the growth of childhood ALL, providing prolonged survival of mice engrafted with ALL. We conclude that RAD001 warrants clinical investigation as a combination therapy for relapsed ALL and potentially as front-line therapy for relatively chemotherapy-resistant ALL subgroups.

Acknowledgments

The authors thank Dr Julius Juarez, as well as Stephanie Hackworthy and Craig Godfrey (Westmead Animal Care Facility, Sydney, Australia), for technical support for the in vivo experiments; Tamra Cox and Aysen Yuksel for preparation of histologic tissue sections; Hong Yu (Electron Microscopy Laboratory, Westmead Research Hub, Sydney, Australia), for technical assistance with the electron microscopy; Karen Byth for assistance with statistical analysis of results; John Ray for assistance with pharmacokinetic/pharmacodynamic analysis; and Novartis Institutes for Biomedical Research, Oncology (Basel, Switzerland) for providing RAD001 for these experiments.

This work was supported by the Children's Cancer Aid Society Südtirol Regenbogen (Bressanone, Italy), the National Health and Medical Research Council (Canberra, Australia; project grant 352326), and Leukemia & Lymphoma Society (White Plains, NY; grant 6105-08). L.J.B. was supported by a Fellowship from the Cancer Institute New South Wales (Sydney, Australia).

Authorship

Contribution: R.C. and J.H. designed and performed experiments, analyzed data, and contributed to writing the manuscript; A.C., R.B., and M.T. performed experiments and analyzed data; K.F.B. supported research and contributed to writing the manuscript; and L.J.B. supported

research, designed experiments, analyzed data, and contributed to writing the manuscript

Conflict-of-interest disclosure: The authors declare no competing financial interests.

Correspondence: Linda J. Bendall, Westmead Institute for Cancer Research, Westmead Millennium Institute, Darcy Rd, Westmead, NSW 2145, Australia; e-mail: linda_bendall@wmi.usyd.edu.au.

References

1. Pui C, Relling M, Campana D, Evans W. Childhood acute lymphoblastic leukemia. Rev Clin Exp Hematol. 2002;6:161-180.
2. Einsiedel H, von Stackelberg A, Hartmann R, et al. Long-term outcome in children with relapsed ALL by risk-stratified salvage therapy: results of trial acute lymphoblastic leukemia-relapse study of the Berlin-Frankfurt-Münster Group 87. J Clin Oncol. 2005;23:7942-7950.
3. Dow L, Martin P, Moohr J, et al. Evidence for clonal development of childhood acute lymphoblastic leukemia. Blood. 1985;66:902-907.
4. Bertrand F, Spengemen J, Shelton J, McCubrey J. Inhibition of PI3K, mTOR and MEK signaling pathways promotes rapid apoptosis in B-lineage ALL in the presence of stromal cell support. Leukemia. 2005;19:98-102.
5. Wang L, Fortney J, Gibson L. Stromal cell protection of B-lineage acute lymphoblastic leukemic cells during chemotherapy requires active Akt. Leuk Res. 2004;28:733-742.
6. Juarez J, Baraz R, Gaundar S, Bradstock K, Bendall L. Interaction of interleukin-7 and interleukin-3 with the CXCL-12-induced proliferation of B cell progenitor acute lymphoblastic leukemia. Haematologica. 2007;92:450-459.
7. Avellino R, Romano S, Parasole R, et al. Rapamycin stimulates apoptosis of childhood acute lymphoblastic leukemia cells. Blood. 2005;106:1400-1406.
8. Mabuchi S, Altomare D, Cheung M, et al. RAD001 inhibits human ovarian cancer cell proliferation, enhances cisplatin-induced apoptosis, and prolongs survival in an ovarian cancer model. Clin Cancer Res. 2007;13:4261-4270.
9. Peponi E, Drakos E, Reyes G, Leventaki V, Rassidakis G, Medeiros L. Activation of mammalian target of rapamycin signaling promotes cell cycle progression and protects cells from apoptosis in mantle cell lymphoma. Am J Pathol. 2006;169:2171-2180.
10. Teachey D, Obzut D, Cooperman J, et al. The mTOR inhibitor CCI-779 induces apoptosis and inhibits growth in preclinical models of primary adult human ALL. Blood. 2006;107:1149-1155.
11. Yee K, Zeng Z, Konopleva M, et al. Phase I/II study of the mammalian target of rapamycin inhibitor Everolimus (RAD001) in patients with relapsed or refractory hematologic malignancies. Clin Cancer Res. 2006;12:5165-5173.
12. Zeng Z, Sarbassov dos D, Samudio I, et al. Rapamycin derivatives reduce mTORC2 signaling and inhibit AKT activation in AML. Blood. 2007;109:3509-3512.
13. Dann S, Thomas G. The amino acid sensitive TOR pathway from yeast to mammals. FEBS Lett. 2006;580:2821-2829.
14. Thomas G. mTOR and cancer: reason for dancing at the crossroads? Curr Opin Genet Dev. 2006;16:78-84.
15. Vignot S, Faivre S, Aguirre D, Raymond E. mTOR-targeted therapy of cancer with rapamycin derivatives. Ann Oncol. 2005;16:525-537.
16. Yu K, Toral-Barza L, Discafani C, et al. mTOR, a novel target in breast cancer: the effect of CCI-779, an mTOR inhibitor, in preclinical models of breast cancer. Endocr Relat Cancer. 2001;8:249-258.
17. Khariwala S, Kjaergaard J, Lorenz R, Van Lente F, Shu S, Strome M. Everolimus (RAD) inhibits in vivo growth of murine squamous cell carcinoma (SCC VII). Laryngoscope. 2006;116:814-820.
18. Ito D, Fujimoto K, Mori T, et al. In vivo antitumor effect of the mTOR inhibitor CCI-779 and gemcitabine in xenograft models of human pancreatic cancer. Int J Cancer. 2006;118:2337-2343.
19. Grünwald V, DeGraffenried L, Russel D, Friedrichs W, Ray R, Hidalgo M. Inhibitors of mTOR reverse doxorubicin resistance conferred by PTEN status in prostate cancer cells. Cancer Res. 2002;62:6141-6145.
20. Goudar R, Shi Q, Hjelmeland M, et al. Combination therapy of inhibitors of epidermal growth factor receptor/vascular endothelial growth factor receptor 2 (AEE788) and the mammalian target of rapamycin (RAD001) offers improved glioblastoma tumor growth inhibition. Mol Cancer Ther. 2005;4:101-112.
21. Pui C, Evans W. Treatment of acute lymphoblastic leukemia. N Engl J Med. 2006;354:166-178.
22. Bendall LJ, Kortlepel K, Gottlieb DJ. Human acute myeloid leukemia cells bind to bone marrow stroma via a combination of beta 1 and beta 2 integrin mechanisms. Blood. 1993;82:3125-3132.
23. Juarez J, Dela Pena A, Baraz R, et al. CXCR4 antagonists mobilize childhood acute lymphoblastic leukemia cells into the peripheral blood and inhibit engraftment. Leukemia. 2007;21:1249-1257.
24. Bendall L, Baraz R, Juarez J, Shen W, Bradstock K. Defective p38 mitogen-activated protein kinase signaling impairs chemotaxic but not proliferative responses to stromal-derived factor-1alpha in acute lymphoblastic leukemia. Cancer Res. 2005;65:3290-3298.
25. Khan N, Bradstock K, Bendall L. Activation of Wnt/beta-catenin pathway mediates growth and survival in B-cell progenitor acute lymphoblastic leukaemia. Br J Haematol. 2007;138:338-348.
26. Steinherz P, Gaynon P, Breneman J, et al. Cytoreduction and prognosis in acute lymphoblastic leukemia—the importance of early marrow response: report from the Childrens Cancer Group. J Clin Oncol. 1996;14:389-398.
27. Aguirre D, Boya P, Bellet D, et al. Bcl-2 and CCND1/CDK4 expression levels predict the cellular effects of mTOR inhibitors in human ovarian carcinoma. Apoptosis. 2004;9:797-805.
28. Cao Y, Klionsky D. Physiological functions of Atg6/Beclin 1: a unique autophagy-related protein. Cell Res. 2007;17:839-849.
29. Schrappe M, Camitta B, Pui C, et al. Long-term results of large prospective trials in childhood acute lymphoblastic leukemia. Leukemia. 2000;14:2193-2194.
30. Mabuchi S, Altomare D, Connolly D, et al. RAD001 (Everolimus) delays tumor onset and progression in a transgenic mouse model of ovarian cancer. Cancer Res. 2007;67:2408-2413.
31. Kahan B, Wong R, Carter C, et al. A phase I study of a 4-week course of SDZ-RAD (RAD) quiescent cyclosporine-prednisone-treated renal transplant recipients. Transplantation. 1999;68:1100-1106.
32. Kovarik J, Noe A, Berthier S, et al. Clinical development of an everolimus pediatric formulation: relative bioavailability, food effect, and steady-state pharmacokinetics. J Clin Pharmacol. 2003;43:141-147.
33. Laplanche R, Meno-Tetang G, Kawai R. Physiologically based pharmacokinetic (PBPK) modeling of everolimus (RAD001) in rats involving nonlinear tissue uptake. J Pharmacokinet Pharmacodyn. 2007;34:373-400.
34. Cao C, Subhawong T, Albert J, et al. Inhibition of mammalian target of rapamycin or apoptotic pathway induces autophagy and radiosensitizes PTEN null prostate cancer cells. Cancer Res. 2006;66:10040-10047.
35. Borgmann A, Baldy C, von Stackelberg A, et al. Childhood ALL blasts retain phenotypic and genotypic characteristics upon long-term serial passage in NOD/SCID mice. Pediatr Hematol Oncol. 2000;17:635-650.
36. Liem N, Papa R, Milross C, et al. Characterization of childhood acute lymphoblastic leukemia xenograft models for the pre-clinical evaluation of new therapies. Blood. 2004;103:3905-3914.
37. Teachey D, Sheen C, Hall J, et al. mTOR inhibitors are synergistic with methotrexate: an effective combination to treat acute lymphoblastic leukemia. Blood. 2008;112:2020-2023.
38. Roman-Gomez J, Jimenez-Velasco A, Castillejo J, et al. Promoter hypermethylation of cancer-related genes: a strong independent prognostic factor in acute lymphoblastic leukemia. Blood. 2004;104:2492-2498.
39. Zhou M, Gu L, Findley H, Jiang R, Woods W. PTEN reverses MDM2-mediated chemotherapy resistance by interacting with p53 in acute lymphoblastic leukemia cells. Cancer Res. 2003;63:6357-6362.
40. Wendel H, Malina A, Zhao Z, et al. Determinants of sensitivity and resistance to rapamycin-chemotherapy drug combinations in vivo. Cancer Res. 2006;66:7639-7646.
41. Sun S, Rosenberg L, Wang X, et al. Activation of Akt and eIF4E survival pathways by rapamycin-mediated mammalian target of rapamycin inhibition. Cancer Res. 2005;65:7052-7058.
42. Grossel M, Hinds P. From cell cycle to differentiation: an expanding role for cdk6. Cell Cycle. 2006;5:266-270.
43. Gao N, Zhang Z, Jiang B, Shi X. Role of PI3K/AKT/mTOR signaling in the cell cycle progression of human prostate cancer. Biochem Biophys Res Commun. 2003;310:1124-1132.
44. Gao N, Flynn D, Zhang Z, et al. G1 cell cycle progression and the expression of G1 cyclins are regulated by PI3K/AKT/mTOR/p70S6K1 signaling in human ovarian cancer cells. Am J Physiol Cell Physiol. 2004;287:C281-C291.
45. Brown V, Fang J, Alcorn K, et al. Rapamycin is active against B-precursor leukemia in vitro and in vivo, an effect that is modulated by IL-7-mediated signaling. Proc Natl Acad Sci U S A. 2003;100:15113-15118.
46. Gozuacik D, Kimchi A. Autophagy as a cell death and tumor suppressor mechanism. Oncogene. 2004;23:2891-2906.
47. Wei G, Twomey D, Lamb J, et al. Gene expression-based chemical genomics identifies rapamycin as a modulator of MCL1 and glucocorticoid resistance. Cancer Cell. 2006;10:331-342.
48. Gómez-Santos C, Ferrer I, Santidrián A, Barrachina M, Gil J, Ambrosio S. Dopamine induces autophagic cell death and alpha-synuclein increase in human neuroblastoma SH-SY5Y cells. J Neurosci Res. 2003;73:341-350.
49. Yu L, Wan F, Dutta S, et al. Autophagic programmed cell death by selective catalase degradation. Proc Natl Acad Sci U S A. 2006;103:4952-4957.